Spin-Peierls transition in dimerized stacks of anion-radical salt (N-Me-2,5-di-Me-Pz)(TCNQ), (Pz is pyrazine)

A. Radváková, D.V. Ziolkovskiy, V.O. Cheranovskii, A. Feher, M. Kajňaková, O.N. Kazheva, G.G. Alexandrov, O.A. Dyachenko, V.A. Starodub

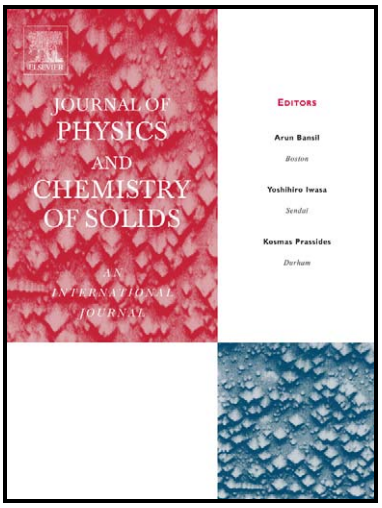

www.elsevier.com/locate/jpcs

Spin-Peierls transition in dimerized stacks of anion-radical salt (N-Me-2,5-di-Me-Pz)$(TCNQ)_2$, (Pz is pyrazine)

A. Radváková, D.V. Ziolkovskiy, V.O. Cheranovskii, A. Feher, M. Kajňaková, O.N. Kazheva, G.G. Alexandrov, O.A. Dyachenko, V.A. Starodub

PII: S0022-3697(09)00250-9
DOI: doi:10.1016/j.jpcs.2009.09.004
Reference: PCS 5942

To appear in: *Journal of Physics and Chemistry of Solids*

Received date: 4 March 2009
Revised date: 9 July 2009
Accepted date: 4 September 2009

Cite this article as: A. Radváková, D.V. Ziolkovskiy, V.O. Cheranovskii, A. Feher, M. Kajňaková, O.N. Kazheva, G.G. Alexandrov, O.A. Dyachenko and V.A. Starodub, Spin-Peierls transition in dimerized stacks of anion-radical salt (N-Me-2,5-di-Me-Pz)$(TCNQ)_2$, (Pz is pyrazine), *Journal of Physics and Chemistry of Solids*, doi:10.1016/j.jpcs.2009.09.004

Spin-Peierls Transition in Dimerized Stacks of Anion-Radical Salt (N-Me-2,5-di-Me-Pz)$(TCNQ)_2$, (Pz is pyrazine)

A. Radváková[1(a)], D.V. Ziolkovskiy[(b)], V.O. Cheranovskii[(b)], A. Feher[(a)], M. Kajňaková[(a)], O.N. Kazheva[(c)], G.G. Alexandrov[(d)],O.A. Dyachenko[(c)], V.A. Starodub[(e)]

[(a)] Centre of Low Temperature Physics of the Faculty of Science UPJŠ and IEP SAS, Park Angelinum 9, SK-04154 Košice, Slovakia;

[(b)] V. Karazin Kharkov National University, 4 Svobody Sq., 61077 Kharkov, Ukraine;

[(c)] Institute of Problems of Chemical Physics, Russian Academy of Sciences, Semenov av., 1, 142432, Chernogolovka, Russia;

[(d)] N.S.Kurnakov Institute of General and Inorganic Chemistry Russian Academy of Sciences, 119991, Leninskii av., 31, Moscow, Russia;

[(e)] Institute of Chemistry, Jan Kochanowski Univerity, 15 G Świętokrzyska str., 25-406 Kielce, Poland.

Abstract

An anion-radical salt (ARS) (N-Me-2,5-di-Me-Pz)$(TCNQ)_2$, where Pz is pyrazine, was synthesized and its crystal structure was resolved. X-ray diffraction experiments on single crystals were performed. Heat capacity was measured in the temperature range from 2 K to 300 K. Magnetisation and magnetic susceptibility were measured in the temperature range from 2 K to 300 K and the low-temperature part was measured in

[1] Corresponding author, alena.radvakova@upjs.sk, +421 55 234 2314

magnetic fields from 5 mT to 5 T. The experimental results were explained in terms of dimerized Heisenberg spin 1/2 chain model. Numerical calculations were performed and compared with experimental data.

Keywords: A. organic compounds, C. X-ray diffraction, D. magnetic properties, D. specific heat

1. Introduction

Anion-radical salts (ARS) of 7,7,8,8-tetracyanoquinodimethane (TCNQ) were the first organic objects to exhibit metallic properties [1]. In the middle of 80s, conducting ARS of TCNQ were synthesized possessing a unique ability to melt without decomposition [2, 3]. This revealed wide usage possibilities of such ARS in electronics. TCNQ ARS with cations containing an additional donor atom (for instance, pyrazine-based cations), can be used to deposite conducting organic coating over a metallic substrate. In these ARS there is a possibility of additional interactions (besides the electrostatic ones) between anion-radical TCNQ stacks and cations via non-alkylated nitrogen atom of pyrazine (Pz). This may result in structures unusual for TCNQ ARS. Using this approach, we have synthesized for the first time the quasi-two-dimensional TCNQ ARS of (N-Et-Pz)$(TCNQ)_{2.5}$ [4], (N-Et-2,5-di-Me-Pz)$(TCNQ)_2$ composition [5] and (N-Me-NH_2-Pz)$(TCNQ)_2$ with dimeric cation [6].

In our previous paper [7] the structure, optical and magnetic properties of novel ARS (N-Me-2,6-di-Me-Pz)$(TCNQ)_2$ were described. It was shown that this ARS exhibits properties allowing us to describe the system as a spin-ladder (similiar properties have been discovered in ARS (N-Et-Pz)$(TCNQ)_{2.5}$ [8]).

In this paper we present the results of our study of magnetic and thermodynamic properties of isomeric ARS (N-Me-2,5-di-Me-Pz)$(TCNQ)_2$. The optical properties of this ARS were described recently [9]. The crystal structure of this ARS differs considerably from the crystal structure of (N-Me-2,6-di-Me-Pz)$(TCNQ)_2$ [10], although from the chemical point of view they differ only in the position of methyl groups in cation molecule.

X-ray diffraction experiments on single crystals were performed. Heat capacity was measured in the temperature range from 2 K to 300 K. Magnetisation and magnetic susceptibility was measured in the temperature range from 2 K to 300 K and the low-temperature part was measured in magnetic fields from 5 mT to 5 T. We analysed the results of the low-temperature susceptibility and heat capacity investigations. This analysis has indicated that the magnetic system of this salt may be described adequately by dimerised Heisenberg spin 1/2 chain model with alternating exchange.

2. Experimental

Studied ARS was prepared using standard procedure [3]. In order to grow single crystals, recrystallization from acetonitrile was performed.

X-Ray diffraction studies of ARS were carried out with an Enraf Nonius CAD-4 diffractometer, using graphite monochromated Mo-K_α radiation, $\omega/2\theta$-scanning. The crystal and molecular structure was solved by direct method and following Fourier synthesis using the SHELXS-97 program [11]. The structure of ARS was refined by the full-matrix least-squares method against F^2 in anisotropic approximation for all non-hydrogen atoms, using the SHELXL-97 program [12]. The hydrogen atoms positions in ARS were calculated from the geometric conditions. Due to the crystallographic symmetry conditions there is an equal probability that the methyl group CH_3 sits either

on the nitrogen atom N(1) or N(1a). So, in the cation layer cations of two types are present in an equal ratio, differing only in the positions of CH_3-group in cation molecule. The basic crystallographic data are given in Tab. 1. The bond lengths and bond angles are given in Tab. 2.

The magnetisation measurements and magnetic susceptibility measurements were performed in a *Quantum Design* MPMS. The field dependence of magnetisation was measured in the magnetic field from 0 T to 5 T at five different temperatures. The temperature dependence of susceptibility was investigated in the temperature range from 2 K to 300 K and in applied magnetic fields from 5 mT to 5 T. The diamagnetic contribution to the susceptibility was estimated using Pascal's constants [13] and subtracted from the total susceptibility. The temperature dependence of heat capacity was investigated in the temperature range from 2 K to 300 K in zero magnetic field and in applied magnetic field 9 T, using a *Quantum Design* PPMS.

3. Results and discussion

The X-ray analysis shows that the investigated salt has a layered structure, where cation layers alternate along the *c* axis with the layers consisting of TCNQ anion-radicals (Fig.1) [10]. Anions form stacks along the *a* axis, where they are situated in pairs shifted in respect to each other, and characterized by two patterns of overlapping (Fig.2) [10]. Within the pairs the molecules are eclipsed in a higher degree than between the pairs. That's why we can speak about the dimerization of TCNQ in stacks, despite the fact that the interplanar distances within and between the pairs are practically the same, i.e. 3.24 Å and 3.27 Å, respectively.

The fact that there is only one type of TCNQ particles in the crystal structure and that the interplanar distances between them are practically the same, is in good agreement

with the absence of splitting bands in the Raman spectra [9]. Experimental bond lengths in TCNQ molecules were used in the HOSE approach [14] to estimate the charge on anions to be about -0.44 *e*. This value is in a good agreement with the value (-0.51 *e*) estimated from Raman spectra [9]. Both methods, structural and spectroscopic, of the charge determination are approximate (with the error of few percents) and neglect the effects induced by neighboring molecules. So we can state that almost full charge is equally distributed from one cation to two TCNQ particles.

In such a way, the band formed by overlapping of TCNQ π-orbitals, is filled to one quarter and in the consequence of the Peierls transition the period of the TCNQ column should increase four times, corresponding to the creation of tetramers. Nevertheless, in our sample a dimer structure of columns was observed. Dimer has spin S = 1/2 and therefore possible magnetic interactions between dimers lead to the origin of tetramers, which corresponds to the spin-Peierls transition. In this connection we have studied the temperature dependence of heat capacity (Fig.3) and magnetic susceptibility in a wide temperature range (Fig.4).

In order to get the magnetic contribution of the specific heat, we subtracted the lattice part ($C_{lattice}$) of the specific heat from the raw data, using standard assumption that $C_{lattice} \sim T^3$ at low temperatures. We fitted the magnetic part of the specific heat data at low temperatures (up to 8 K) by the expression $C_{magn} = \alpha T^2 \exp[-\beta T^2]$ (so called Maxwell function) (Fig.3), which satisfactorily describes the magnetic part of the heat capacity of analogue systems [7].

The temperature dependent magnetic susceptibility for ARS is reported in Fig.4. It shows a broad maximum centered at $T_{max} \approx 36$ K, which is a typical signature of a low-dimensional $S = 1/2$ spin system. Temperature dependence of effective moment was fitted with the rational function:

$$\mu_{eff} = \frac{P_1 \cdot T}{P_2 + T} \qquad (1)$$

with P_1 = 0.58 μ_B/K and P_2 = 97.32 K. The value of saturated effective moment corresponds to 0.156 unpaired electrons.

Similar dependence of magnetic susceptibility was given from [15, 16]:

$$\chi = \frac{G}{T} \cdot \frac{A + BT^{-1} + CT^{-2}}{1 + DT^{-1} + ET^{-2} + FT^{-3}}, \qquad (2)$$

where A, B, C, D, E and F are a function of coupling constants, G is a fitting parameter. (Fig.5).

Formula (2) corresponds to microscopic description by means of Heisenberg dimerised spin 1/2 chain model. The corresponding Hamiltonian has the form [18]

$$\hat{H} = -J \sum_{i=1}^{n/2} [\hat{S}_{2i} \hat{S}_{2i-1} + \delta \hat{S}_{2i} \hat{S}_{2i+1}], \qquad (3)$$

where J is negative exchange parameter describing antiferromagnetic coupling between neighbor spins of the chain. The parameter δ takes into account the distortion in the chain and can vary from $\delta = 0$ (isolated $TCNQ^-$ dimers) to $\delta = 1$ (a uniform chain of S = 1/2 spins).

We also performed exact diagonalization study of the specific heat and magnetic susceptibility of Heisenberg spin chains formed by 10-16 spins and described by the Hamiltonian (3). By means of branching diagram technique [19] all eigenvalues of the Hamiltonian matrices were determined separately for each subspace with a given value of total spin. For zero magnetic field the exact energy spectra have, for an energy gap Δ between the ground state and the lowest excitation state, due to the finite size of spin chains. It is of interest for the interpretation of experimental data that our numerical simulation shows one peak temperature behaviour of molar magnetic susceptibility χ at

zero or weak magnetic field H and two peak behaviour in the case of sufficiently strong magnetic field, i.e. $2\mu H^* \sim \Delta$ (Fig. 6).

According to general theory of quasi-one dimensional spin-Peierls system at zero magnetic field the round peak of susceptibility should be located at temperature $T_{max} > T_{SP}$, where T_{SP} is the temperature of spin-Peierls transition (SPT). This means that our system has a form of a set of isolated uniform spin chains. For infinite uniform chain in zero magnetic field there are exact estimation of T_{max} and χ_{max} on the base of thermodynamic Bethe ansatz [20, 21] $T_{max} \sim 0.6409J$, $\frac{\chi_{\max} J}{N_A g^2 \mu^2} \approx 0.1469$. To use experimental value $T_{max} \sim 36$ K, $g = 2$ we obtain estimates $J = 56.25$ K and $\chi_{max} \sim 0.00392$ emu/mol, which is close to experimental value 0.0040 emu/mol for fields up to $\approx$ 150 mT. The absence of remain susceptibility at $H \sim 5$mT agrees with the weak dimerization of the infinite spin chain due to SPT because for infinite uniform chain zero field susceptibility at $T \to 0$ takes finite value [20]. From the data shown in Fig. 10 we may estimate the energy gap Δ for triplet excitations of the chain: $\Delta \geq 2\mu H$, where $H \sim 5$mT. In the result we have $\Delta \geq 0.007$ K. According to BCS relation $\frac{\Delta(T=0)}{T_{SP}} \approx 2.47$ from [22] the critical temperature of SPT should have extremely low value ~ 0.003K, which cannot be determined in our experiment.

To explain the experimental data for magnetic field $H > 10$mT let us suppose that the magnetic sublattice of our ARS is a collection of infinite and finite spin chains formed by even number of spins only. Naturally, short spin chains should be dimerized at any temperature due to finite size effects. This proposal does not contradict above analysis for weak magnetic field. Our numerical estimations on the base of exact diagonalization study of dimerized linear chains formed up to 16 spins in magnetic field (Fig.6) and similar results for the finite chains in zero field [17] give rather close values

for the position and height of round peak. On the other side these values also close to the exact estimates for infinite uniform spin chain in zero magnetic field [20]. Thus, according to our numerical calculations for uniform spin chain (δ = 1) with N = 14 the broad maximum appears at $kT = 0.63J$ and for δ = 0.9 we have the broad maximum at $kT = 0.59J$. This corresponds to J = 5.25 meV and χ_{max} ~ 0.00379 emu/mol.

Note, that our suggestion about magnetic structure of ARS is similar to well known "broken chain effect" [23]. The difference between our suggestion and this effect is the absence of paramagnetic contribution due to finite chains with odd number of spins. Simple first order perturbative analysis shows that the formation of one common even fragment from two odd fragments leads to the decrease of total energy similar of recombination of free radicals.

Our numerical simulation shows one peak temperature behavior of molar magnetic susceptibility χ at zero or weak magnetic field H and two peak behavior in case of sufficiently strong magnetic field: $2\mu H \sim \Delta$ (Fig.6), where Δ is the energy gap for triplet excitations of the chain. For $H < H^*$ first sharp peak decreases quickly with the decrease of H. Obviously, such a behavior of magnetic susceptibility is the result of disappearance of the energy gap at $H = H^*$. Thus we may suppose that the second peak of χ appears due to the contribution of finite dimerized spin chains to general susceptibility at sufficiently strong magnetic fields.

There is also the decrease of total magnetic contribution to specific heat due to presence of finite spin chains with different Δ.

We should emphasize that our explanation of the experimental data on the base of oversimplified linear spin chain model is only one of the possible explanations and has qualitative character.

Appearance of two peaks (Fig.9) in the temperature dependence of magnetic susceptibility was proved in our experiments. In Fig.10 the low-temperature susceptibility is shown in dependence on applied magnetic field. As can be seen, at temperatures below 7 K increasing magnetic field leads to the change in the curve slope. Dependence χ(T) in all applied fields can be described, in the temperature range from 10 K to T_{max}, with a simple parabola $\chi(T) = a + bT + cT^2$. Extrapolation to $T = 0$ K allowed us to determine the low-temperature part of magnetic susceptibility $\chi'(T) = \chi_{exp}(T) - (a + bT + cT^2)$, shown in Fig.10.

Peculiarities of the low-temperature susceptibility can not be connected with magnetic impurities because they dependend strongly on applied magnetic field (Fig.10). In fields up to ≈ 50 mT this remain susceptibility practically does not depend on magnetic field and maintains on the level of 10^{-4} emu/mol, while in lower fields it decreases rapidly. Considering the results of theoretical calculations shown in Fig.8 we suppose that in a field close to 0 T only one peak in susceptibility appears and the increase of susceptibility with increasing magnetic field can be related to the appearance of the second peak in intermediate fields, as predicted by theory. Then, from data shown in Fig.10 we can establish the energy gap Δ between the ground state and the lowest excitation state $2\mu H^* \sim \Delta$, where Δ ≈ 0.07 K.

Note also that the temperature dependence of low-temperature susceptibility of dimerized XY spin chain at different values of applied magnetic field was studied theoretically in adiabatic approximation in [24]. In contrast to our simulation the temperature dependence of corresponding susceptibility demonstrated only one peak due to more simple structure of the excitation spectrum of one-dimensional XY model in comparison with Heisenberg spin chain.

Conclusion

The temperature dependence of both magnetic susceptibility and heat capacity can be adequately described by the one-dimensional dimerised Heisenberg spin 1/2 chain. To confirm this interpretation numerical calculations using corresponding Hamiltonian (2) were performed. According to these calculations, the dimerized chain has a strongly field-dependent gap and a second low-temperature peak in susceptibility appears at low magnetic fields ($0 \leq H \leq 500$ mT). Our experimental data are in a good agreement with these calculations and we suppose that in our system there are dimerized spin chains. Below 36 K the dimers couple to tetramers and this corresponds to the spin-Peierls transition.

In magnetic fields above 50 mT the gap closes and this is manifested by the increase of susceptibility at low temperatures. This is a new feature of the spin-Peierls phase behaviour in magnetic field, predicted theoretically and observed experimentally on our genuine organic system (N-Me-2,5-di-Me-Pz)$(TCNQ)_2$.

Acknowledgements

This work was supported by the grants of Slovak Research and Development Agency under the contracts LPP-0102-06, No. APVV-VVCE-0058-07, No. APVV-0006-07 and VEGA – 1/0159/09. The financial support of U.S.Steel – DZ Energetika Košice is acknowledged.

References

1. I. F. Schegolev, Electric and magnetic properties of linear conducting chains, Phys. Stat. Sol. Ser. A 12 (1972) 9 - 45.
2. M. Tanaka, F. Urano, M. Nakabata., Jap. Pat. 60-139832 (1987).

3. V.A. Starodub, V.V. Barabashova, Ye.M. Gluzman et al., USSR Pat. 1389226 (1987).

4. D.V. Ziolkovskiy, A.V. Kravchenko, V.A. Starodub, O.N. Kazheva, A.V. Khotkevich, Crystalline and molecular structure of novel anion-radical salt (N-Et-Pz)$(TCNQ)_3$ (Pz is pyrazine), Functional Materials 12 (2005) 577 - 582.

5. D.V. Ziolkovskiy, O.N. Kazheva, G.V. Shilov, O.A. Dyachenko, A.V. Kravchenko A.V. Khotkevich, V.A. Starodub, A novel anion-radical salt (N-Et-2,5-di-Me-Pz)$(TCNQ)_2$ (Pz is pyrazine), Functional Materials 13 (2006) 119 - 124.

6. O.N. Kazheva, D.V. Ziolkovskiy, G.G. Alexandrov, A.N. Chekhlov, O.A. Dyachenko, V.A. Starodub, A.V. Khotkevich, Crystal and molecular structure of the new anion-radical salts – (N-Me-2-NH_2-Pz)$(TCNQ)_2$ and (N-Me-Tetra-Me-Pz)$(TCNQ)_2$ (Pz is pyrazine), Synthetic Metals 156 (2006) 1010 - 1016.

7. A.Radvakova, D.V. Ziolkovskiy, A. Feher, M. Kajnakova, B. Barszcz, A. Graja, V.A. Starodub, Quasi-two-dimensional ARS (N-Me-2,6-di-Me-Pz)$(TCNQ)_2$, Pz is Pyrazine), submitted to Journal of Physics: Condensed Matter.

8. A. Lapinski, M. Golub, V.A. Starodub., Proc. of the 10th Int. Conf. ERPOS, Cargese, 2005 p. A 094.

9. B. Barszcz, A. Graja, D. V. Ziolkovskiy, V. A. Starodub, Spectral properties of the TCNQ anion radical salt (N-Me-2,5-$(Me)_2$-Pz)$(TCNQ)_2$, Synthetic Metals 158 (2008) 246 - 250.

10. O.N. Kazheva, D.V. Ziolkovskiy, G.G. Alexandrov, O.A. Dyachenko, V.A. Starodub, A.V. Khotkevich, G.Y. Vasilets, Crystal and molecular structure of the new anion-radical salts (N-Me-2,6-di-Me-Pz)$(TCNQ)_2$ and (N-Me-2,6-di-Me-Pz)$(TCNQ)_2$ (Pz is pyrazine), Functional Materials 13 (2006) 1 - 6.

11. G.M. Sheldrick, SHELXS-97, University of Gottingen, Germany, 1997

12. G.M. Sheldrick, SHELXL-97, University of Gottingen, Germany, 1997

13. J.C. O'Connor, Magnetochemistry – Advances in Theory and Experimentation, Progress in Inorganic Chemistry. N.Y.: Stephen J. Loppard, (1982) 209 P.

14. T.M. Krycowski, Crystallographic studies and physicochemical properties of p-electron compounds. Stabilization energy and the Kekule contributions derived from experimental bond length, R. Anuliewicz, Acta Crystallogr. B 39 (1983) 732 - 739.

15. J.W. Hall, W.E. Marsh, R.R. Weller, W.E. Hatfield., Exchange Coupling in the Alternating-Chain Compounds catena-Di-μ-chloro-bis(4-methylpyridine)copper(II), catena-Di-μ-bromo-bis(N-methylimidazole)copper(II), catena-[Hexanedione bis(thiosemicarbazonato)copper(II), and catena-[Octanedione bis(thiosemicarbazonato)copper(II), Inorg. Chem. 20 (1981) 1033 - 1037.

16. Ballester, A.M. Gil, A. Gutierrez, M.F. Perpiñán, M.T. Azcondo, A.E. Sánchez, C. Marzin, G. Tarrago, C. Bellitto, Supramolecular Architecture and Magnetic Properties of Copper(II) and Nickel(II) Porphyrinogen-TCNQ Electron-Transfer Salts, Chem. Eur. J. 8 (2002) 2539 - 2548.

17. T. Barnes, J. Riera, Susceptibility and excitation spectrum of $(VO)_2P_2O_7$ in ladder and dimer-chain model, Phys. Rev. B 50 (1994) 6817 - 6822.

18. J.C. Bonner, M.E. Fisher, Linear Magnetic Chains with Anisotropic Coupling Phys. Rev. 135 (1964) A640 – A658

19. V.O. Cheranovskii, Matrix elements of the spin Hamiltonian, Teor. Experim. Himiya 20 (1984) 468 - 472.

20. A. Klumper, D.C. Johnston, Thermodynamics of the Spin-1/2 Antiferromagnetic Uniform Heisenberg Chain, Physical Review Letters 84 (2000) 4701- 4704.

21. D.C. Johnston, R.K. Kremer, M. Troyer, X. Wang, A. Klumper, S.L. Buď ko, A.F. Panchula, P.C. Canfield, Thermodynamics of spin S = 1/2 antiferromagnetic uniform

and alternating-exchange Heisenberg chains, Physical Review B 61 (2000) 9558 - 9606.

22. E.Orignac, R. Chitra, Mean-field theory of the spin-Peierls transition, Physical Review B 70 (2004) 214436.

23. Y.Liu, J.E.Drumheller, R.D.Willett, Low-temperature of the quasi-one-dimensional spin-1/2 Heisenberg antiferromagnets (6MAP)$CuCl_3$ and (3MAP)$CuCl_3$: Spin-Peierls transition versus broken-chain effects, Physical Review B 52 (1995) 15327.

24. R. de Lima, C. Tsallis, Magnetic field influence on the spin-Peierls instability in the quasi-one-dimensional magnetostrictive XY model: Thermodynamical properties, Phys.Rev. B 27 (1983) 6896 - 6915.

Figure captions

Fig. 1. Fragment of crystal structure of the (N-Me-2,5-di-Me-Pz)$(TCNQ)_2$.

Fig. 2. Overlapping of TCNQ anion-radicals in (N-Me-2,5-di-Me-Pz)$(TCNQ)_2$.

Fig. 3. Approximation of low-temperature part of molar heat capacity (open circles) with formula $C_{tot} = \alpha T^2 \exp[-\beta T^2] + \gamma T^3$, $\alpha = 7.90 \cdot 10^{-3}$, $\beta = 6.96 \cdot 10^{-3}$, $\gamma = 1.422 \cdot 10^{-2}$ (solid line).

Fig. 4. Temperature dependence of magnetic susceptibility measured in zero-field cooling regime (ZFC) in the field 100 mT (open circles) and 1 T (triangles). Inset: temperature dependence of effective moment (points) fitted with rational function (1) (solid line).

Fig. 5. Magnetic susceptibility fitted with Heisenberg linear chain model, spin-ladder model proposed by Barnes and Riera [17] and spatially isotropic 2d Heisenberg antiferromagnetic (HAF) square lattice model.

Fig. 6. Theoretical prediction for temperature and field dependences of magnetic susceptibility for a) 14 spins and b) 16 spins.

Fig. 7. Experimental data of magnetic susceptibility (open circles) in field 5 mT compared to theoretical prediction (solid line) for $h = 0$.

Fig. 8. Experimental data of heat capacity measured in the field 0 T (stars) and 9 T (open circles) compared to theoretical predictions for h = 0 (solid line) and h = 1 (dashed line).

Fig. 9 a) Temperature dependence of magnetic susceptibility in fields from 5 mT to 150 mT, and b) temperature dependence of magnetic susceptibility in fields from 200 mT to 5 T.

Fig. 10. Field dependence of low-temperature tail of magnetic susceptibility data at temperature 3 K in fields from 5 mT to 150 mT, inset shows dependence in fields up to 5 T.

Table 1. Crystal data and structure refinement for (N-Me-2,5-di-Me-Pz)$(TCNQ)_2$ (**1**).

Compound	(**1**)
Empiric formula	$C_{31}H_{19}N_{10}$
Formula weight	531.56
Crystal system	Triclinic
Space group	$P\ \bar{1}$
a/Å	7.218(1)
b/Å	7.909(2)
c/Å	13.433(3)
α/°	81.30(3)
β/°	84.27(3)
γ/°	65.36(3)
U/Å^3	688.4(2)
Z	1
λ/Å	0.71073
D_{calc}, /g cm^{-3}	1.28
μ/mm^{-1}	0.082
Number of reflections collected	3177
Number of independent reflections	2410
Number of reflections with $[F_0 > 4\sigma(F_0)]$	1221
Number of parameters refined	203
R	0.056
$(2\theta)_{max}$, °	49.96

Interval for h	$-8 \leq h \leq 2$
Interval for k	$-9 \leq k \leq 9$
Interval for l	$-15 \leq l \leq 15$

Table 2. Bond distances (Å) and bond angles (°) in (N-Me-2,5-di-Me-Pz)$(TCNQ)_2$ (**I**)

N(1)-C(1)	1.345(5)
N(1)-C(2)	1.324(4)
N(1)-C(3)	1.423(8)
N(2)-C(5)	1.146(4)
N(3)-C(6)	1.148(4)
N(4)-C(15)	1.136(4)
N(5)-C(16)	1.144(4)
C(1)-C(2)#1	1.367(5)
C(1)-C(4)	1.461(5)
C(2)-C(1)#1	1.367(5)
C(5)-C(7)	1.420(4)
C(6)-C(7)	1.419(4)
C(7)-C(8)	1.382(4)
C(8)-C(13)	1.433(4)
C(8)-C(9)	1.434(4)
C(9)-C(10)	1.344(4)
C(10)-C(11)	1.435(4)
C(11)-C(14)	1.393(4)
C(11)-C(12)	1.432(4)
C(12)-C(13)	1.348(4)
C(14)-C(16)	1.423(4)
C(14)-C(15)	1.425(4)

C(2)-N(1)-C(1)	119.3(3)
C(2)-N(1)-C(3)	118.6(5)
C(1)-N(1)-C(3)	121.8(5)
N(1)-C(1)-C(2)#1	117.3(3)
N(1)-C(1)-C(4)	121.0(4)
C(2)#1-C(1)-C(4)	121.6(4)
N(1)-C(2)-C(1)#1	123.4(3)
N(2)-C(5)-C(7)	179.6(4)
N(3)-C(6)-C(7)	178.5(3)
C(8)-C(7)-C(6)	121.5(3)
C(8)-C(7)-C(5)	122.4(3)
C(6)-C(7)-C(5)	116.1(3)
C(7)-C(8)-C(13)	121.3(3)
C(7)-C(8)-C(9)	121.5(2)
C(13)-C(8)-C(9)	117.2(3)
C(10)-C(9)-C(8)	121.6(3)
C(9)-C(10)-C(11)	121.3(3)
C(14)-C(11)-C(12)	121.2(3)
C(14)-C(11)-C(10)	121.7(3)
C(12)-C(11)-C(10)	117.1(3)
C(13)-C(12)-C(11)	121.7(3)
C(12)-C(13)-C(8)	121.1(3)
C(11)-C(14)-C(16)	122.2(3)
C(11)-C(14)-C(15)	122.4(3)
C(16)-C(14)-C(15)	115.3(3)

N(4)-C(15)-C(14)	179.0(3)
N(5)-C(16)-C(14)	179.6(3)

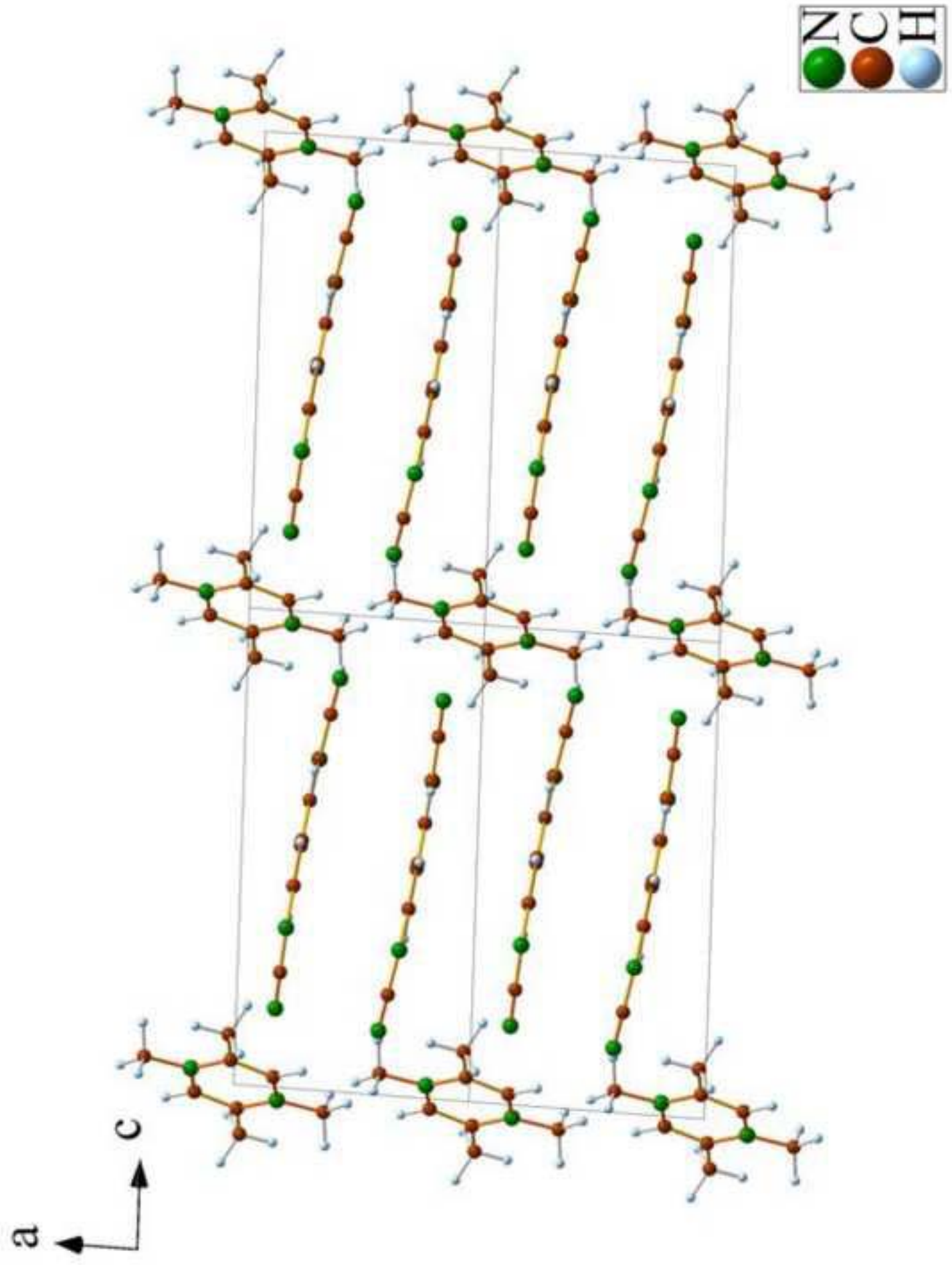

Figure

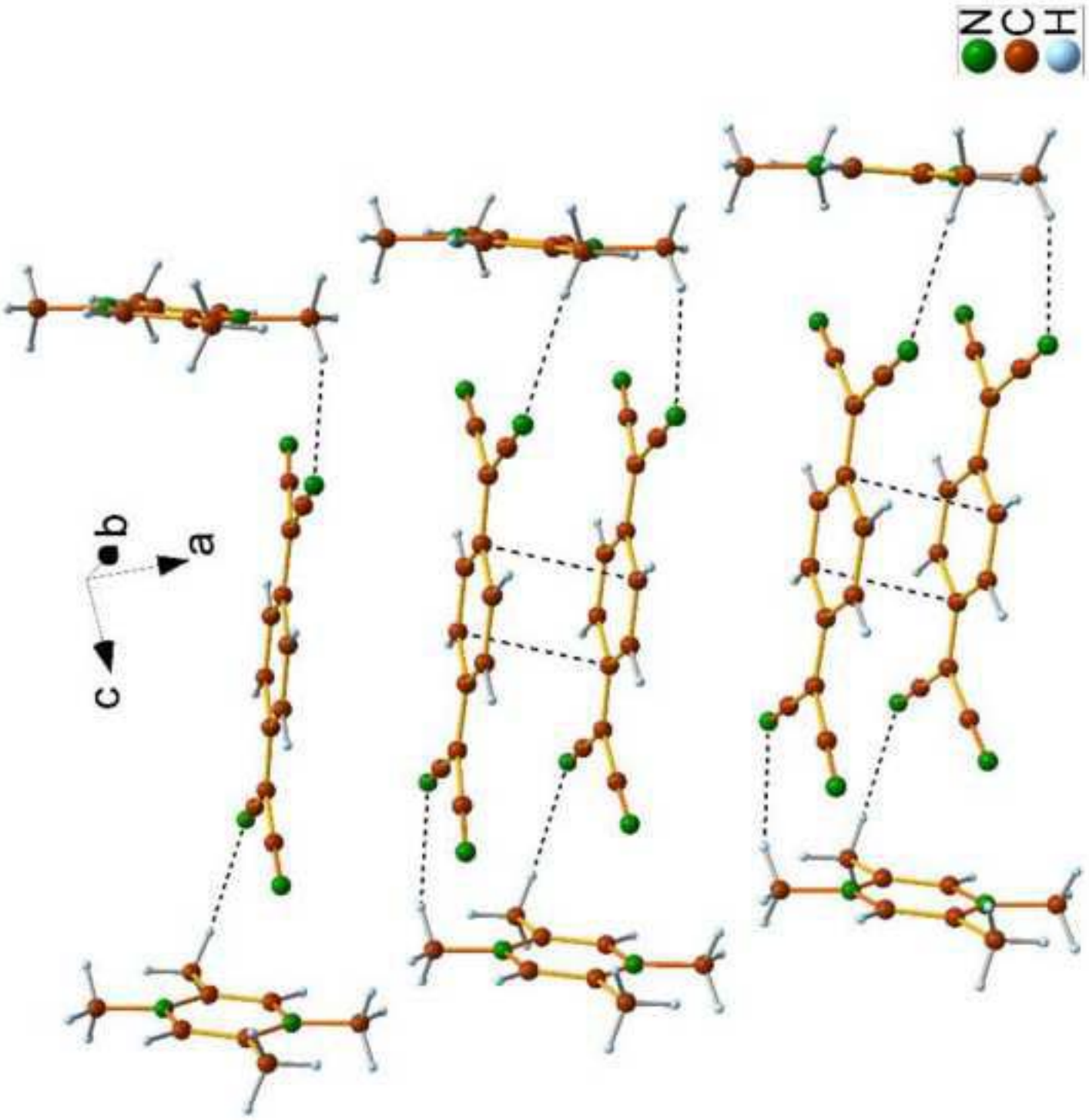

Figure

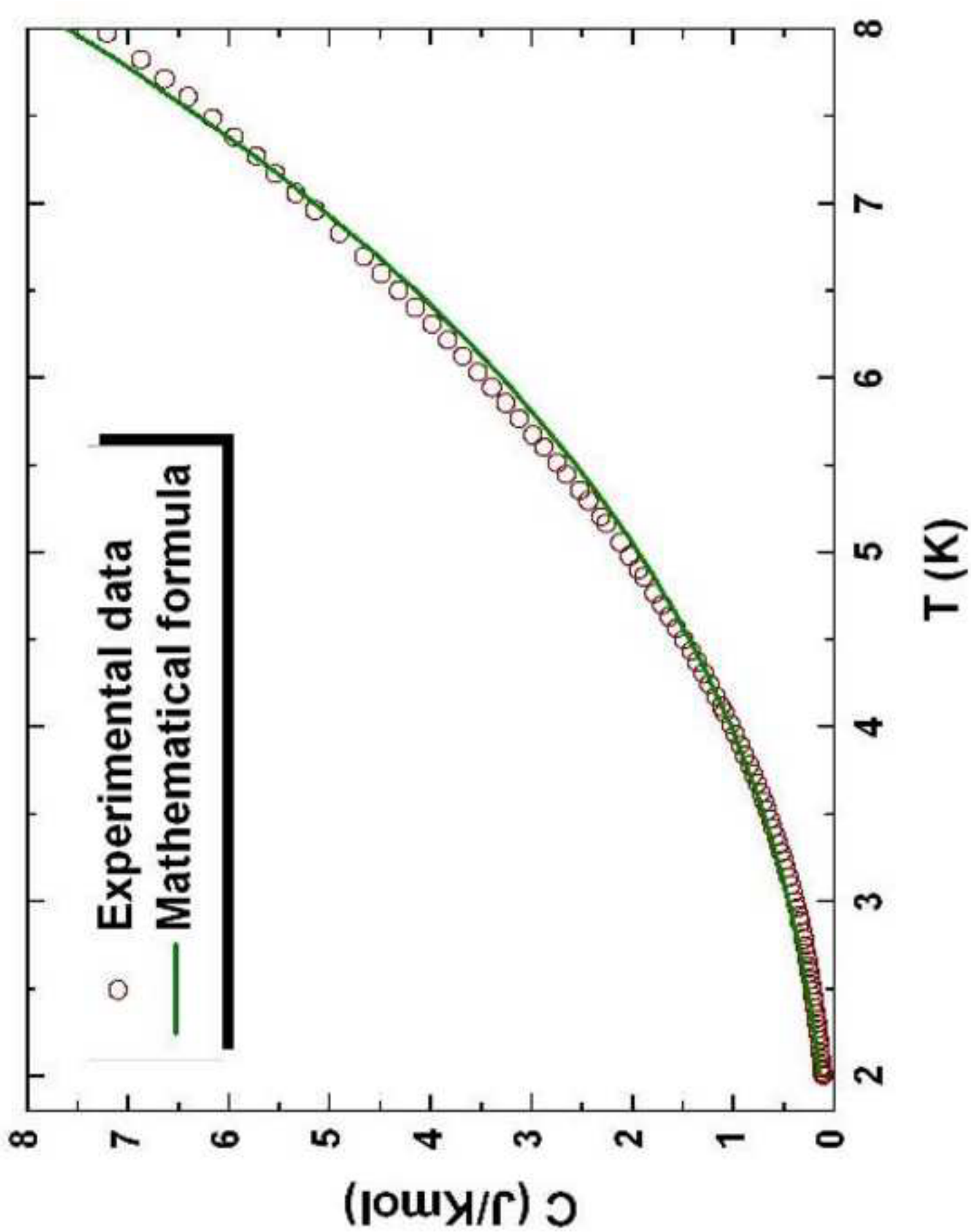

Figure

Figure

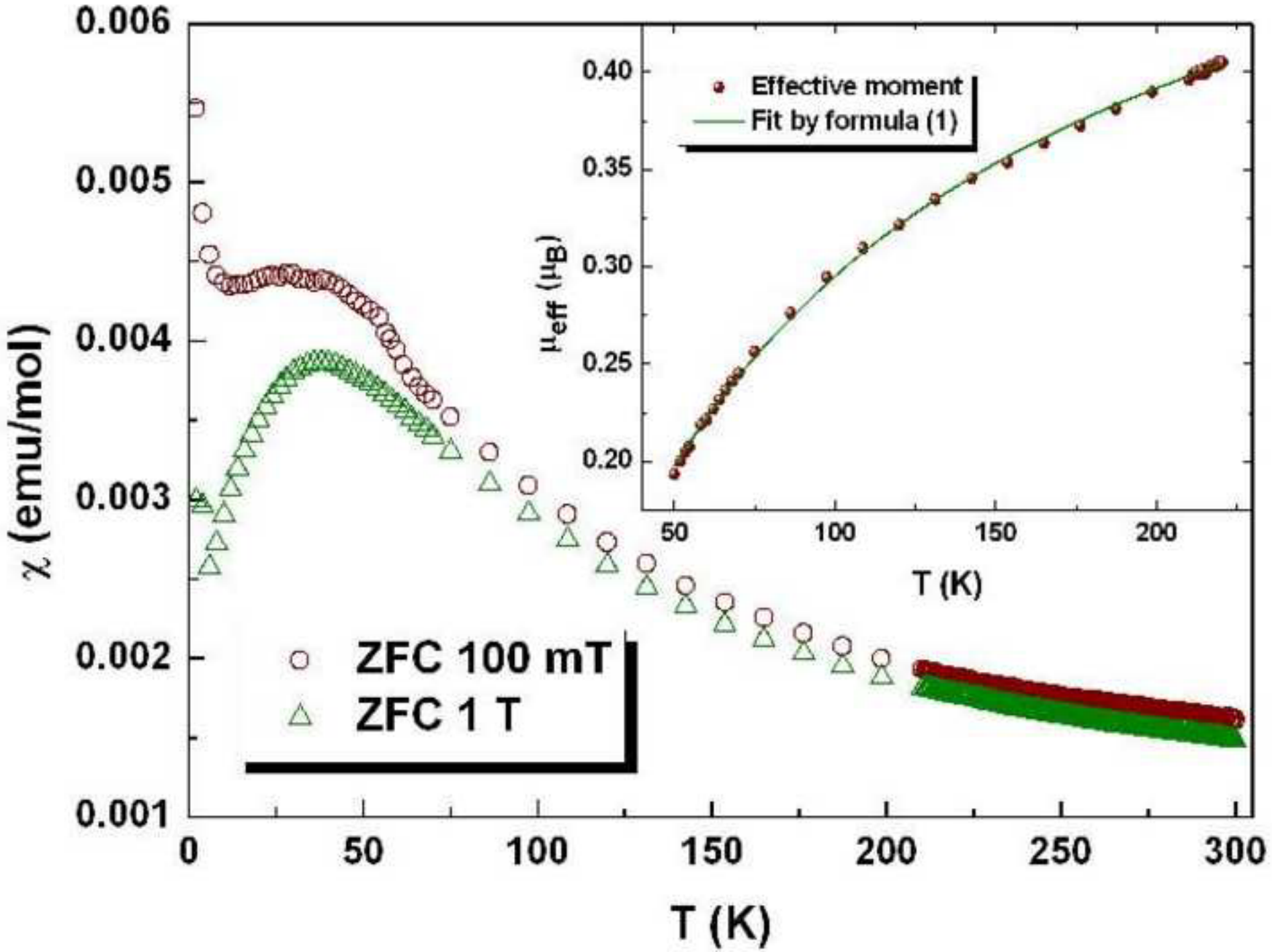

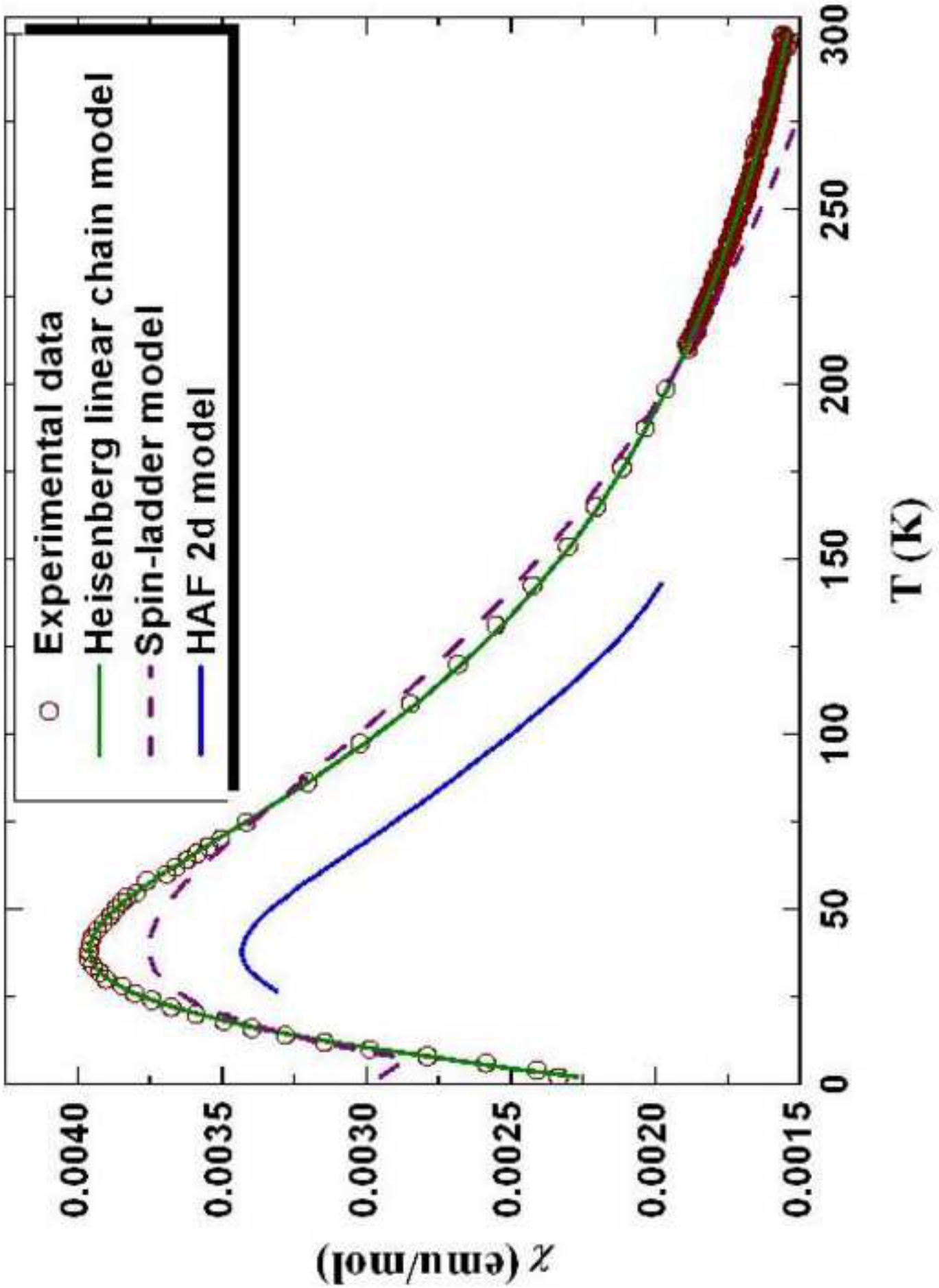

Figure

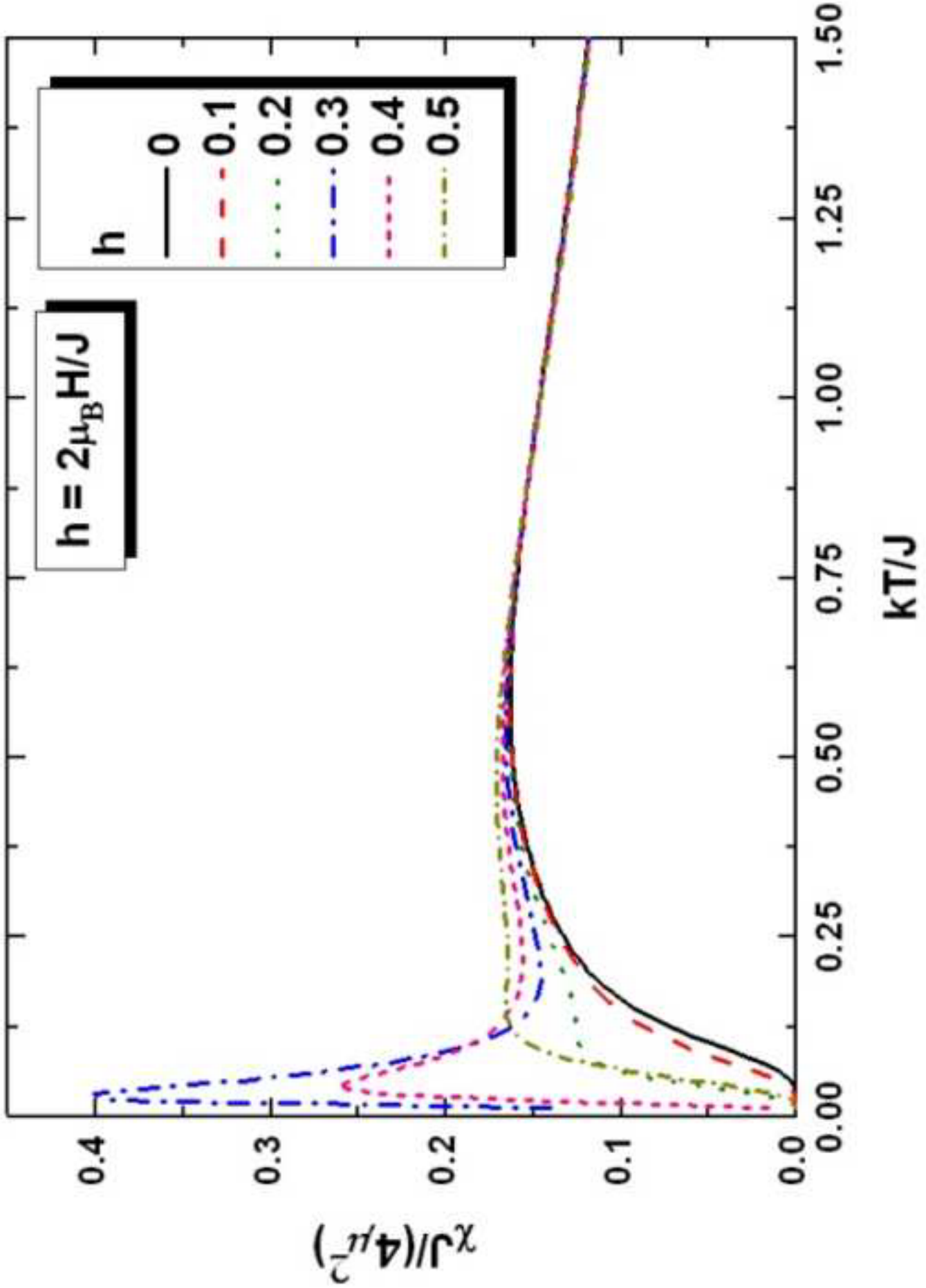

Figure(s)

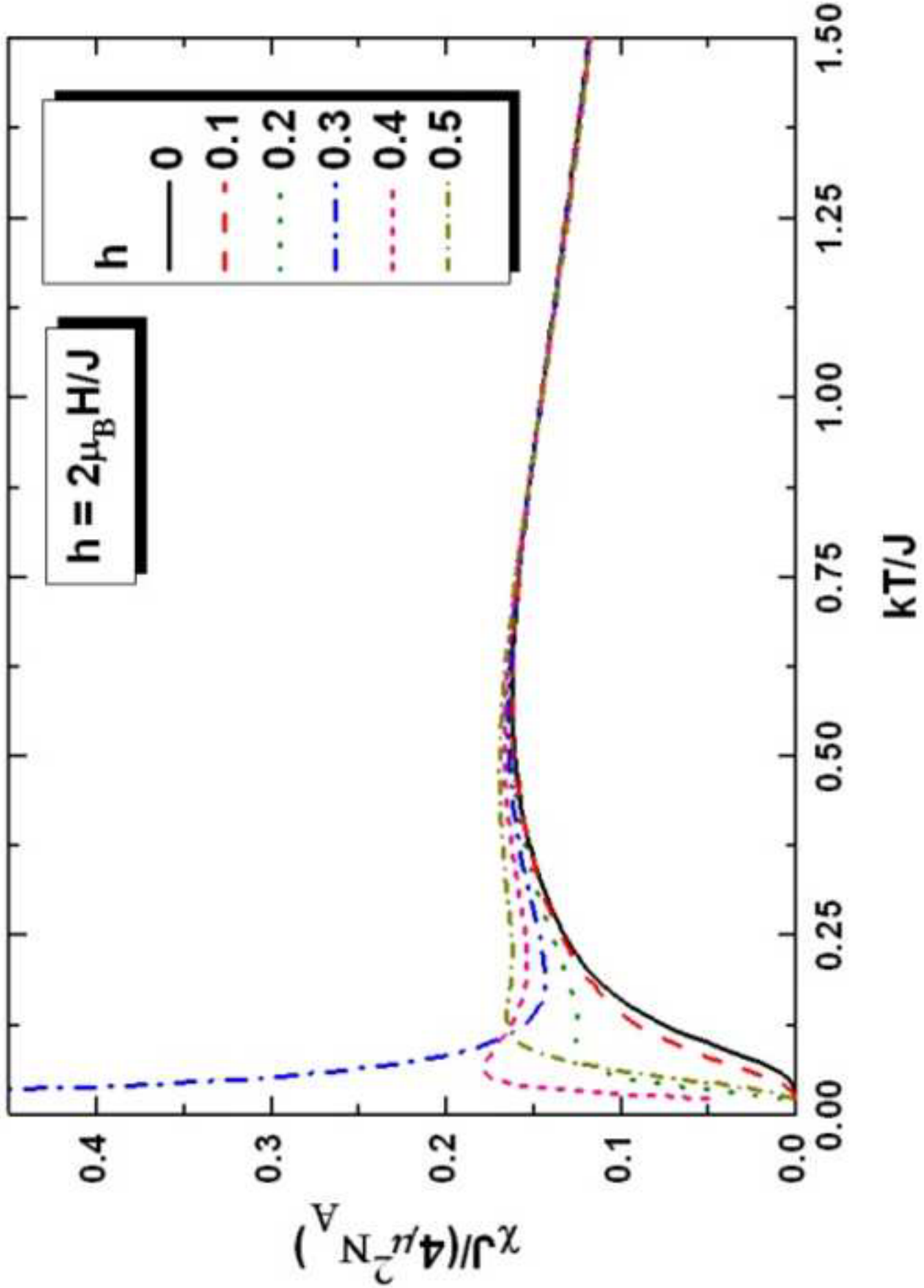

Figure(s)

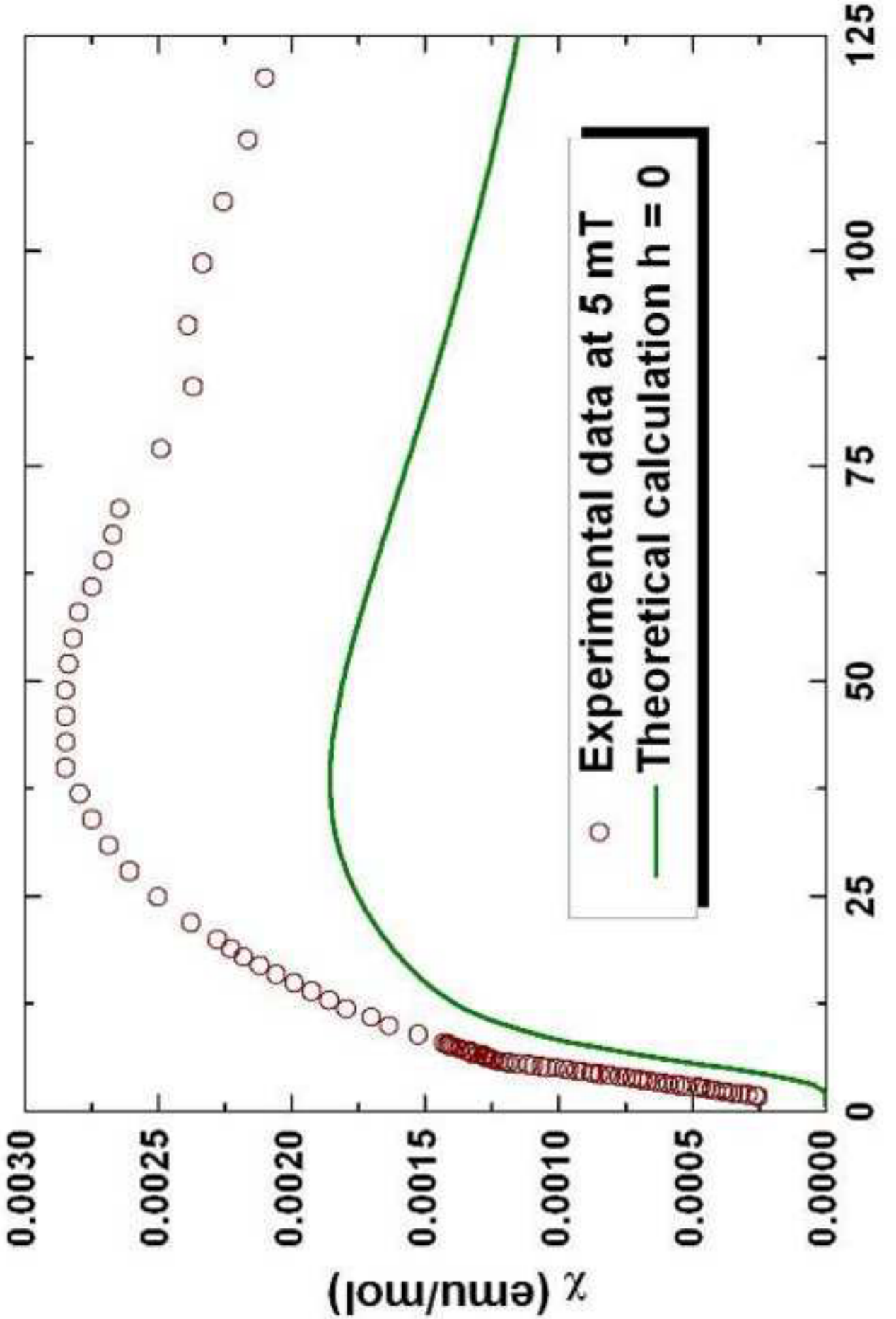

Figure

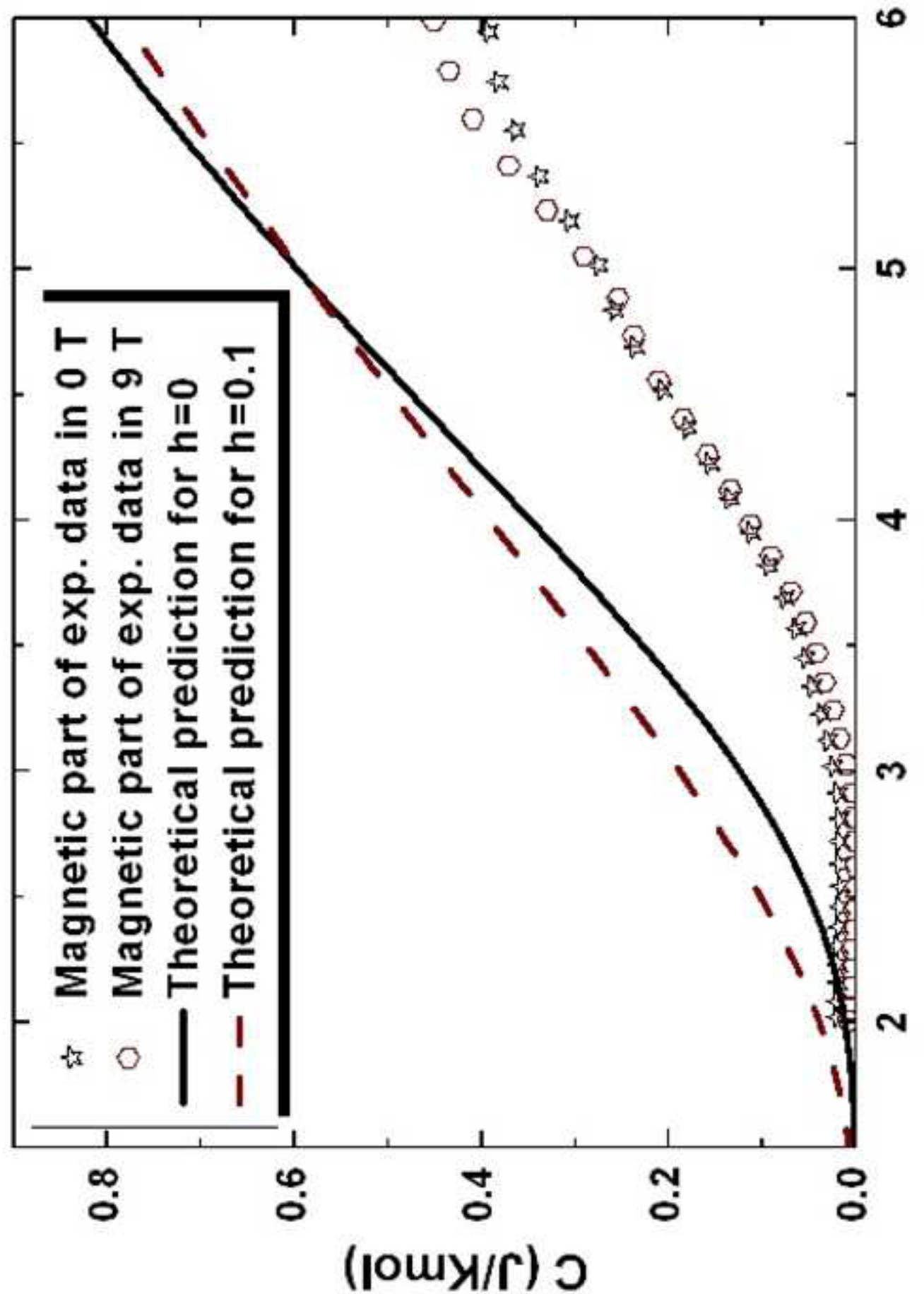

Figure

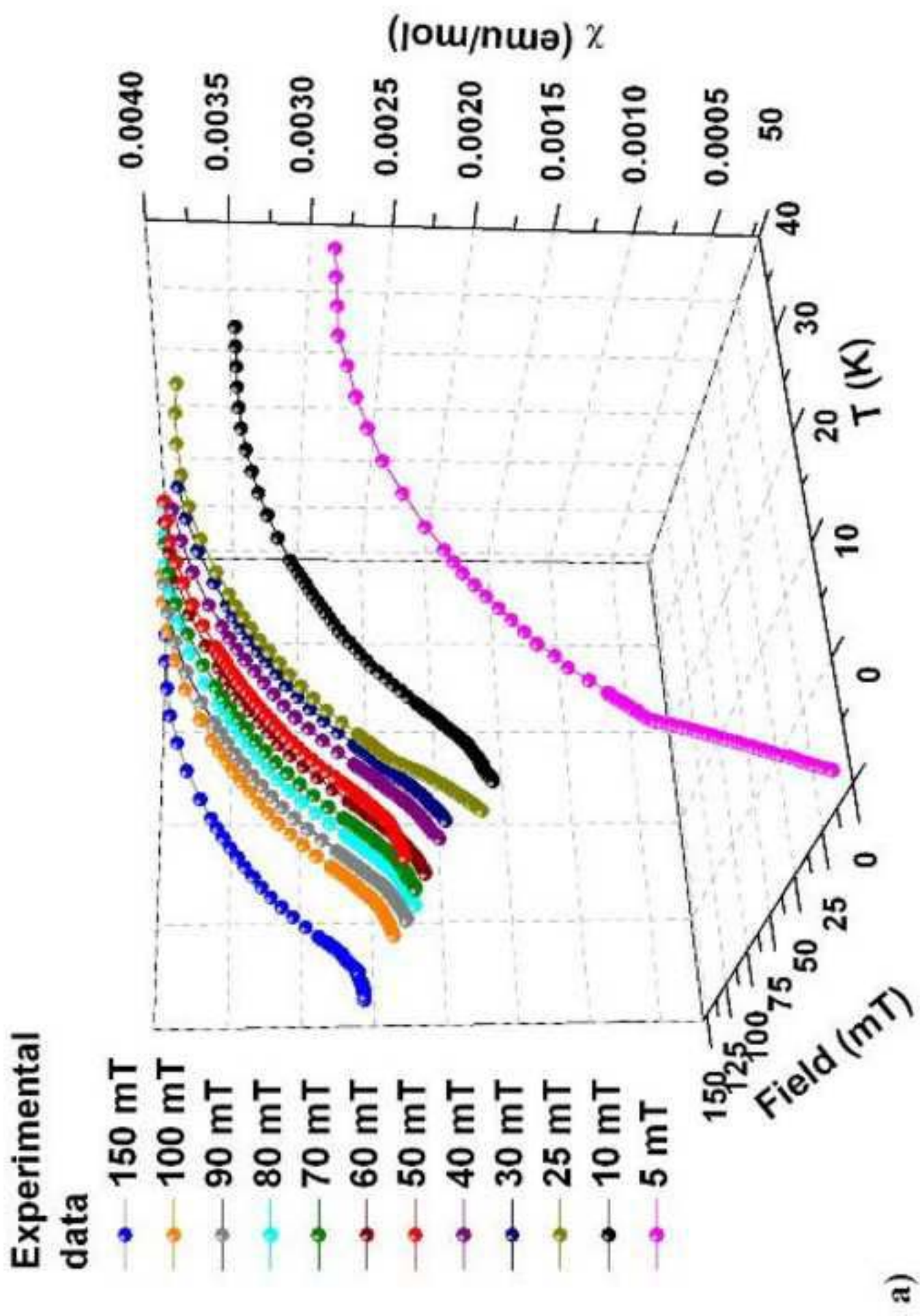

Figure

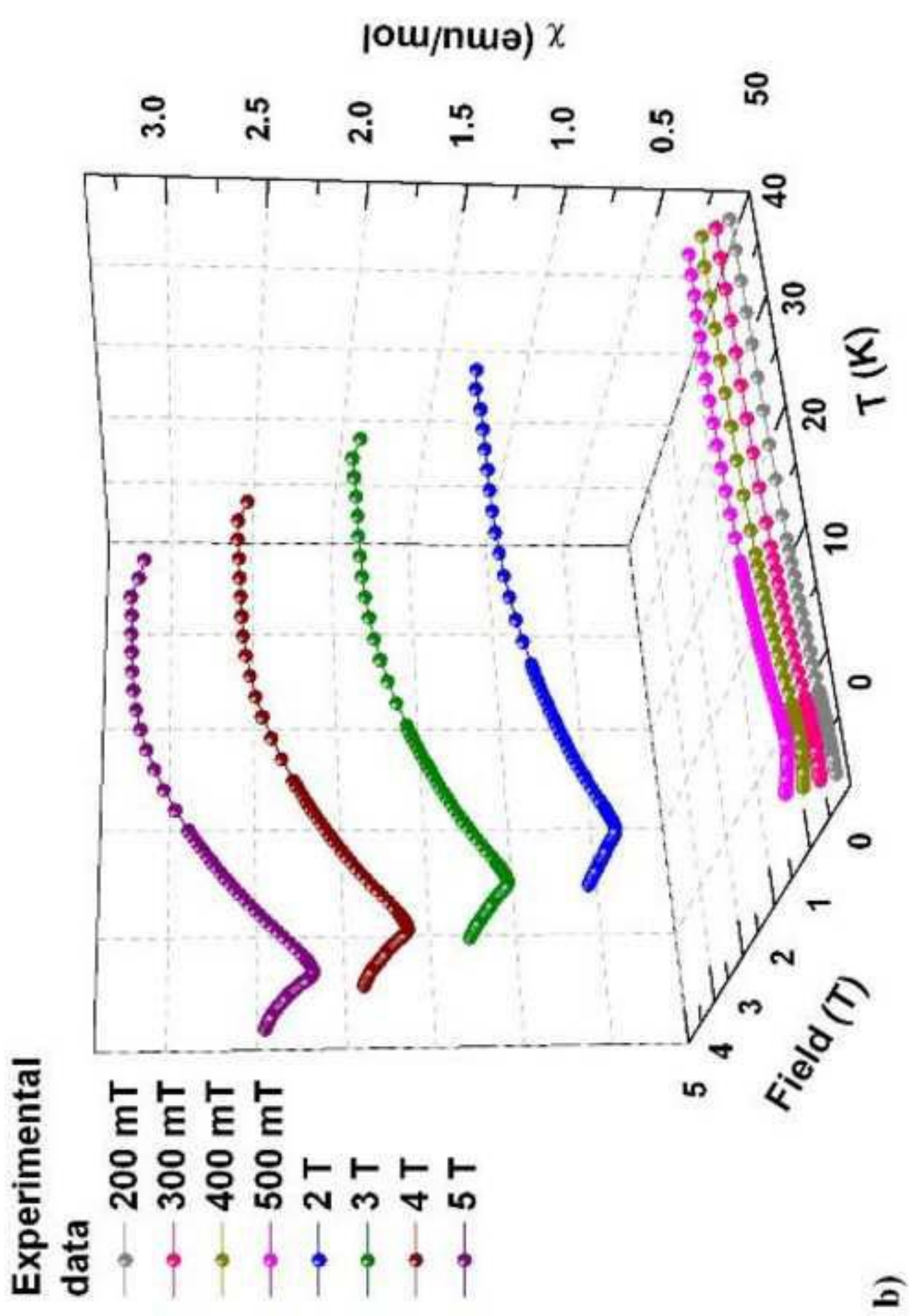

Figure

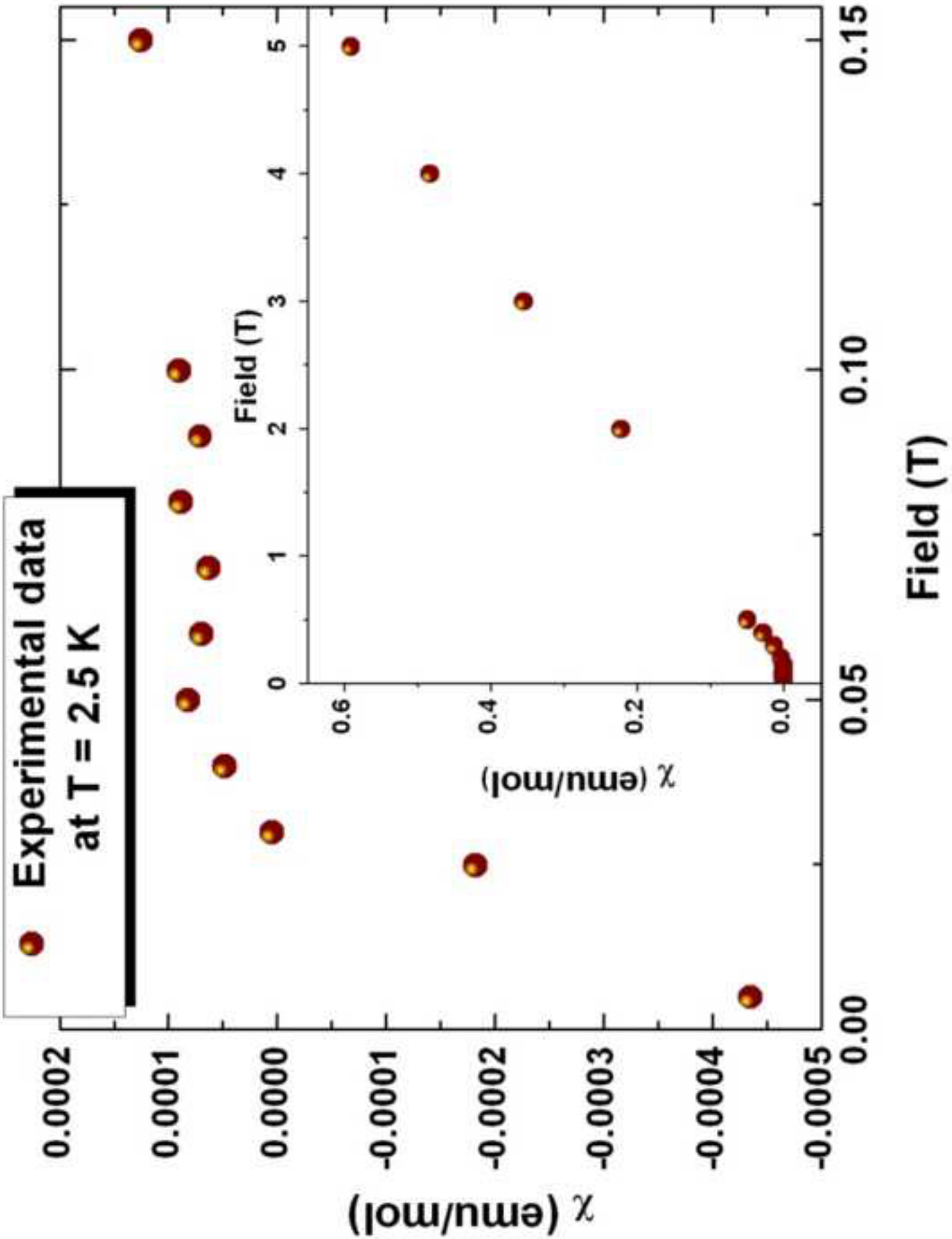

Figure(s)